Tight gas fracturing productivity calculation model based on gas-water permeability curve

Jing Tang, Longjiang Li *, Fanmao Ye, Chuan Liu

Southwest Petroleum University, Chengdu, 610000, China

* Corresponding Author Email: 201931012437@stu.swpu.edu.cn

Abstract. Measuring well production per well can not only simplify the process flow, improve economic efficiency, but also reduce the development cost of the oil field. In this paper, a single-well measurement of oil well production is carried out by establishing a capacity calculation model for fracturing straight wells in tight gas reservoirs by means of gas-water phase infiltration curve. According to different permeability and porosity, several representative relative permeability curves are selected for normalization treatment, and then the angle-preserving transformation principle is used, considering the formation stress sensitivity effect and gas slip effect, as well as the stress sensitivity effect in the fracture and the effect of high-speed non-Daxi effect on gas seepage, the quasi-pressure function is introduced, and the capacity calculation model of the fracturing straight well of the tight gas reservoir is established, so as to achieve the calculation of the yield.

Keywords: phase infiltration curve, normalization, fracturing straight well production.

1. Gas-water phase infiltration curve

1.1. Experimental principle

The experiment was tested by non-steady-state method, and the test method refers to the oil and gas industry standard SY/T5345-1999.The calculation formula of relative permeability and saturation derived from Berkeley's leading edge displacement theory, and the experimental data are processed, and the relationship curve of relative permeability and saturation can be obtained. According to Darcy's law, various fluids related to formation stress damage are injected under laboratory conditions, or seepage conditions are changed, and the permeability change of the core is measured to evaluate the degree of reservoir permeability damage.

1.2. Experimental equipment process and experimental results

The gas-water relative permeability stress-sensitive experimental instrument is also mainly divided into core part, injection part and extraction part.

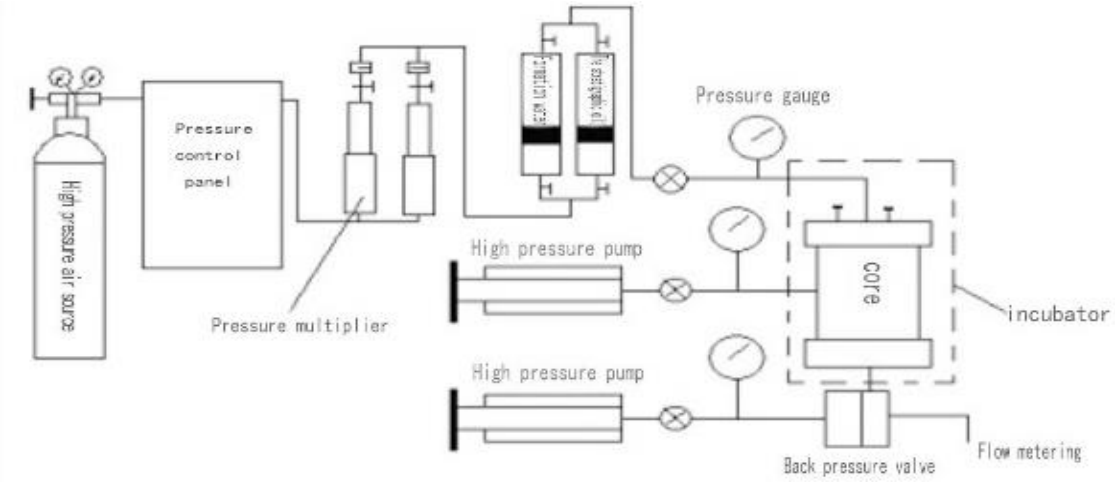

Figure 1. Flowchart of stress-sensitive experimental device with gas-water two-phase permeability.

Analysis of test results:

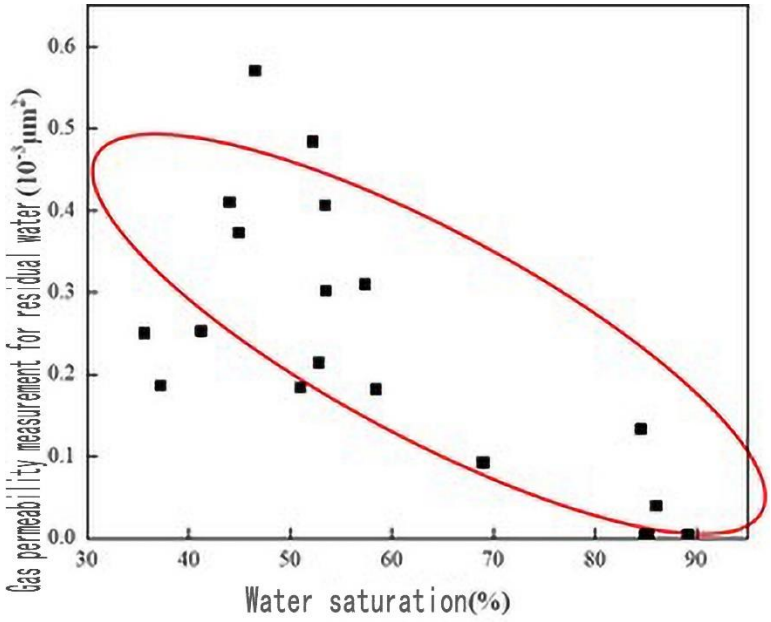

Figure 2. Scatter plot of gas permeability with water saturation change.

Table 1. Statistical table of test data.

Sample number	Gas permeability(10^{-3}μm^2)	Residual water saturation(%)	Gas phase permeability with residual water (10^{-3}μm^2)
2-61/66	0.726	85.26571114	0.005015757
3-47/195	0.499	84.47769389	0.1333947
3-74/195	1.08	84.9	0.00436
3-165/195	0.444	68.9	0.0925
3-171/195	0.508	58.4	0.182
4-11/168	0.497	37.2	0.186
4-20/168	1.24	53.4	0.406
4-27/168	2.07	52.2	0.484
4-31/168	0.91	35.6	0.25
4-35/168	1.33	44	0.41
4-41/168	1.24	44.9	0.373
4-49/168	0.971	52.8	0.214
4-54/168	1.01	41.2	0.253
5-18/133	0.544	89.1	0.00516
5-98/133	0.528	86	0.0395
6-78/155	0.896	53.5	0.302
6-84/155	0.538	51	0.184
6-86/155	1.19	57.3	0.31
6-90/155	1.54	46.5	0.57
7-70/103	0.444	69.1	0.0926

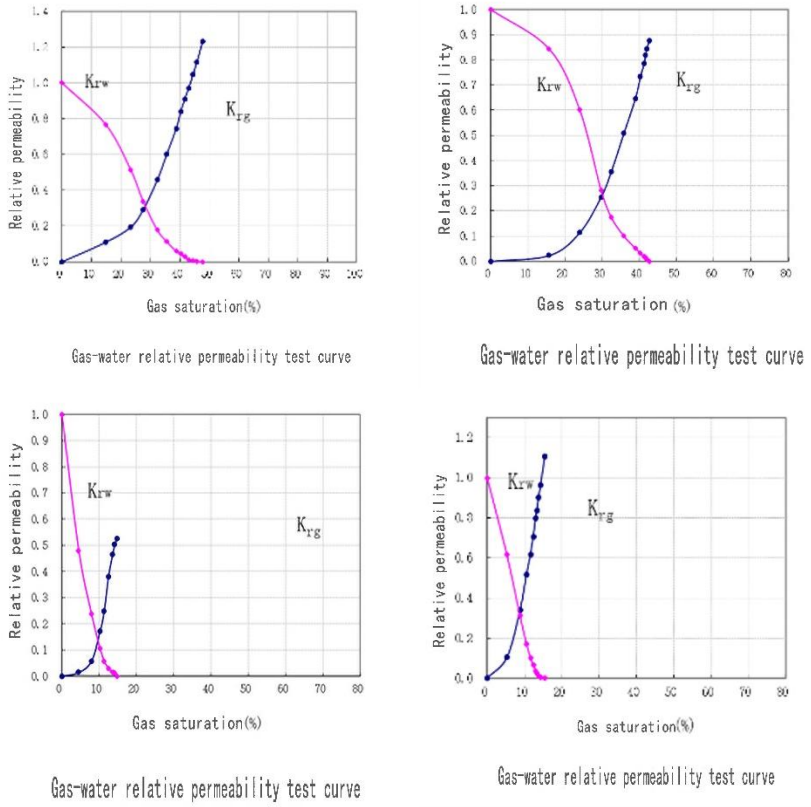

Figure 3. Test curve of sample deed tax relative permeability

As can be seen from the figure, as the saturation of water content in the pore increases, the gas phase permeability of the tight sandstone reservoir decreases sharply.

1.3. Normalization of the relative permeability curve

According to the characteristics of the gas reservoir, according to the different permeability and porosity, several representative relative permeability curves are selected. On this basis, normalization is carried out to obtain an average relative permeability curve that can represent the gas reservoir.

$$\mathrm{K}_{rw}^{*} = (S_w^{*})^{a} \tag{1}$$

$$\mathrm{K}_{rg}^{*} = (1 - S_w^{*})^{b} \tag{2}$$

The standardized relative permeability of gas and water is defined as follows:
Thereinto:

$$\mathrm{K}_{\mathrm{rw}}^{*} = \mathrm{K}_{rw} / \mathrm{K}_{rw}(S_{gr}) \tag{3}$$

$$\mathrm{K}_{\mathrm{rg}}^{*} = \mathrm{K}_{rg} / \mathrm{K}_{rg}(S_{wi}) \tag{4}$$

$$S_w^{*} = (S_w - S_{wi}) / (1 - S_{wi} - S_{gr}) \tag{5}$$

The relationship between the logarithm of the normalized relative permeability of gas and water and the effective wet saturation can be taken on both sides of the above formula, respectively, to obtain:

$$Lg\mathrm{K}_{rw}^{*} = aLgS_w^{*} \tag{6}$$

$$Lg\mathrm{K}_{rg}^{*} = bLg(1 - S_w^{*}) \tag{7}$$

Push it:

$$K_{rw} = K_{rw}^{*} \cdot K_{rw}(S_{gr}) \tag{8}$$

$$K_{rg} = K_{rg}^{*} \cdot K_{rg}(S_{wi}) \tag{9}$$

$$S_w = S_w^{*}(1 - S_{wi} - S_{gr}) + S_{wi} \tag{10}$$

Where:

K_{rw}^{*}, K_{rg}^{*} —Indicates the relative permeability of standardized water and gas, decimal;

K_{rw}, K_{rg} —Indicates the relative permeability of water and gas, decimal;

$K_{rw}(S_{gr}), K_{rg}(S_{wi})$ —The relative permeability of the water under the saturation of the residual gas and the relative permeability of the gas under the saturation of the bound water are represented, respectively, and the decimal number;

S_w, S_{wi}, S_{gr} —Indicates water saturation, bound water saturation, residual gas saturation, decimals, respectively;

S_w^{*} —Normalized moisture saturation, decimal;

a, b—Constants that depend on the pore structure and wettability.

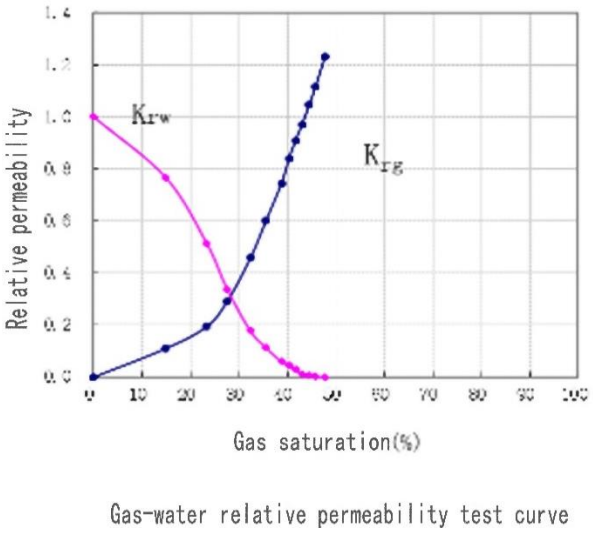

Figure 4. Normalized relative permeability change curve of gas and water two phases.

From Figure 4, it can be seen that the influence of water saturation on the gas phase flow in dense sandstone is much greater than the effect on the gas phase flow in medium and high sandstone. Low-permeability tight sandstone gas reservoirs are more sensitive to water. The low-permeability dense core bore is small in the throat, and the throat passage is the main seepage channel. When water floods gas, the original bondage water in the core is mainly left in the form of a dispersed water film on the throat wall of the tiny hole. After the intrusion of the aqueous phase, it first enters the tiny orifice throat, and before forming a continuous aqueous phase with the bound water film and occupying the seepage channel, the gas is still a single-phase seepage, so the relative permeability of the gas phase is large. When the saturation of the water content increases, the water film begins to thicken, due to the influence of the water film, the gas phase osmosis flow channel becomes narrower, the gas phase permeability begins to decrease sharply, and the water phase permeability slowly increases.When the continuous aqueous phase flows and occupies the seepage channel, the water phase permeability increases rapidly with the increase of water content saturation, the gas phase permeability is further reduced, and finally the residual gas is formed, which can be seen from the figure that the residual gas saturation is low.

2. Fracturing straight well capacity study

2.1. Fracturing straight well capacity forecasting model

The production of fracturing straight wells will cause elliptical flow in the formation, and the vertical cracks formed after the fracturing of the straight well will affect the seepage of gas in the formation, thus forming an elliptical flow with the fracture endpoint as the focus. Using the solution idea of horizontal well plane elliptic flow, the vertical fracture is equivalent to a horizontal well, and the angle-preserving transformation method is introduced to solve it. Since the elliptical seepage in the horizontal plane caused by the introduction of the angle-preserving transformation is equivalent to the plane radial flow of the straight well, so first establish the straight well seepage equation before applying it to the vertical fracture well. The straight well is fractured to form a longitudinal fracture, and in the longitudinal fracture, the confluence effect has less effect on the seepage of the gas, so only the linear flow of the gas is considered in the fracture.

2.2. Model application examples

Reservoir matrix permeability of the target block:0.025~4mD, effective sand width 50~200m, length 500~2000m, formation pressure coefficient:0.87, closed stress gradient:0.013~0.015MPa/m, Reservoirs are divided into three categories according to porosity size: class I reservoirs, Φ>10%, class II reservoirs,7%<Φ<10%, class III reservoirs, 5%<Φ<7%.

Capacity simulations for different types of reservoirs under different fracture parameters are shown in the input parameter table:

Table 2. Crack capacity simulation parameter input table.

Reservoir category	Level III	Level II	Level I
Porosity (%)	5-7	7-10	10
Mean permeability(×10*μm^3)	0.1	0.3	2
Subsurface gas viscosity (mPa.s)	0.018	0.018	0.018
Compression factor of natural gas	0.86	0.86	0.86
Reservoir temperature (℃)	108	108	108
Reservoir pressure (MPa)	29	29	29
Thickness (m)	3	6	9
Combined compressibility(1/MPa)	0.000198	0.000198	0.000198
A deep(m)	3200	3200	3200
Production pressure differential (MPa)	10	10	10
Fracture conductivity(μm^2.cm)	20(30)	20(30)	20(30)

Establish mechanism model of single well post-kill, a total of 57 groups of multi-factor orthogonal experiments were designed, and 90 groups of a single factor influence experiments were designed.

2.3. Analysis of factors affecting fracturing productivity

2.3.1. Stitch length

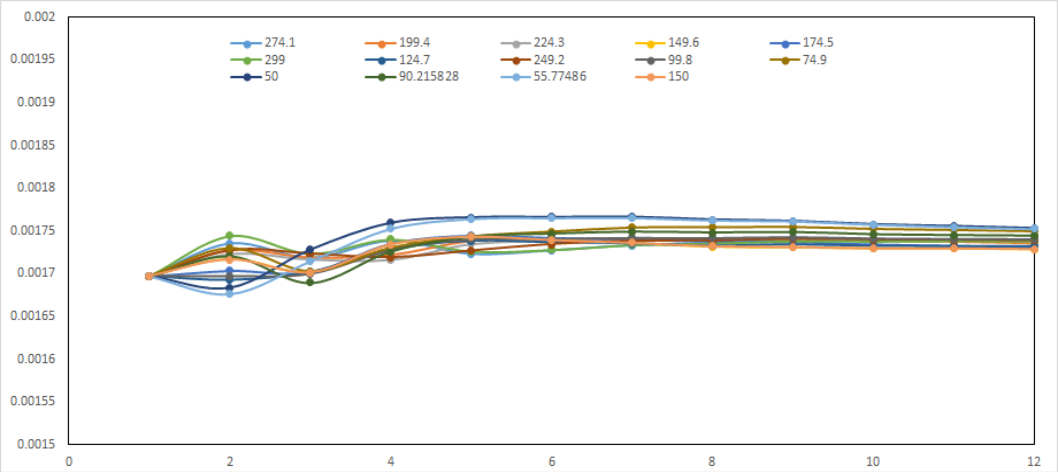

Figure 5. Effect of seam length on yield.

Cracks and a half long: at the beginning of production, the water-gas ratio increases with the increase of fracture half-length, at the end of production, the crack half-length is shorter, the higher the water to air ratio. The fracture half-length should be controlled at 149.6m-299m according to the reservoir type.

2.3.2. Diverting capacity

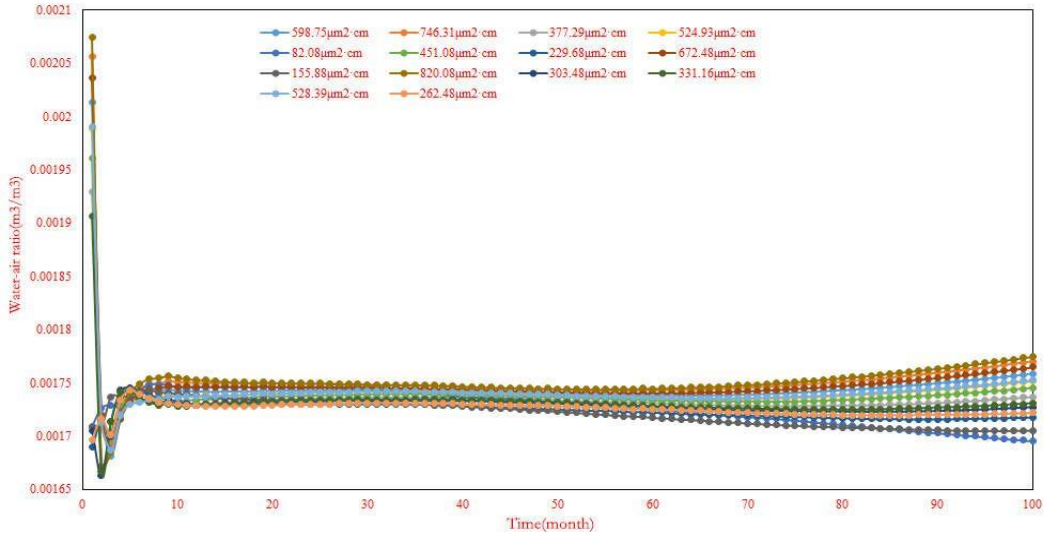

Figure 6. Influence of conductivity on production.

Diverting capacity: the water-gas ratio increases with the increase of conductivity, the smaller the conductivity, the lower the water-gas ratio, and the smaller the variation range. The conductivity should be controlled between 20μm^2.cm to 110μm^2.cm based on the reservoir type.

3. Conclusions and Suggestions

The phase permeability curves are all concave and the relative permeability of gas phase is very low. The water saturation at the isotonic point is about 76%, the bound water saturation is 62.11%, and the water saturation in the gas-water co-permeability area is about 65.90%-96.21%.With the increase of water saturation, the gas phase permeability decreases rapidly, and the relative permeability of water phase rises slowly at the beginning and then increases rapidly, indicating that

the productivity loss of gas Wells is obvious after water is found in gas Wells, and gas Wells are prone to liquid accumulation.

Acknowledgments

This work was financially supported by Sichuan University Student Innovation training program: Development of a block yield prediction software based on machine learning (Project No.: S202110615005) fund.

References

[1] Zhang Jiqiang. Research on reasonable production allocation and stable production capacity of fractured Wells in tight gas reservoirs [D]. Southwest Petroleum University, 2015.

[2] HENG Yong. Study on gas-water distribution law and water control countermeasures based on reservoir architecture analysis [D]. Chengdu University of Technology, 2018.

[3] LIU Li. Experimental study of compound surfactant to reduce water locking effect in low permeability reservoir [D]. Ocean University of China, 2011.

[4] HU Yong. Study on seepage mechanism of tight sandstone gas reservoir [D]. Northeast Petroleum University, 2016.

[5] Huang Yongzhi. Study on gas-water coupling flow law in GB low permeability gas reservoir [D]. Southwest Petroleum University,2018.

[6] Li Yuansheng, Yang Zhixing, Teng Sainan, et al. Prediction of water breakthrough time for edge water gas reservoir considering reservoir dip Angle and water invasion [J]. Petroleum drilling techniques, 2017, 45(01): 91-96.

[7] Hu Yong, Guo Changmin, Xu Xuan, et al. Pore throat structure and seepage characteristics of sandstone gas reservoir [J]. Petroleum geology & experiment,2015,37(03):390-393.

[8] Kai Zhou, Wei Sun, Zheng Wang, et al. Characteristics and influencing factors of tight sandstone reservoir facies permeability in middle Permian He_8-Shan_1member, eastern Sulige Gas Field [J]. Natural gas exploration and development,2016,39(02):31-35+10-11.

[9] Liu Jinshui, Tang Jiancheng. Microscopic pore structure and seepage characteristics of low-permeability reservoir in Xihu Sag and its geological significance: A case study of HY Structure Huagang Formation [J]. China offshore oil and gas, 2013, 25(02): 18-23.

[10] Zhang Jiqiang, Li Xiaoping, Luo Cheng, et al. A new method of calculating post-fractured gas well productivity based on elliptic flow model [J]. Natural gas & oil, 2015, 33(06): 46-50+10-11.